Robotica (2016) volume 34, pp. 2151–2161. © Cambridge University Press 2015
doi:10.1017/S0263574715000223

PD-like controller with impedance for delayed bilateral teleoperation of mobile robots

E. Slawiñski*, S. García, L. Salinas and V. Mut

Instituto de Automática (INAUT), Universidad Nacional de San Juan, Av. Libertador San Martín 1109 (Oeste), J5400ARL San Juan, Argentina

(Accepted February 27, 2015. First published online: April 15, 2015)

SUMMARY

This paper proposes a control scheme applied to the delayed bilateral teleoperation of mobile robots with force feedback in face of asymmetric and time-varying delays. The scheme is managed by a velocity PD-like control plus impedance and a force feedback based on damping and synchronization error. A fictitious force, depending on the robot motion and its environment, is used to avoid possible collisions. In addition, the stability of the system is analyzed from which simple conditions for the control parameters are established in order to assure stability. Finally, the performance of the delayed teleoperation system is shown through experiments where a human operator drives a mobile robot.

KEYWORDS: Bilateral teleoperation; Fictitious force; Force feedback; Mobile robot; PD-like controller; Time delay.

1. Introduction

Robot bilateral teleoperation allows us to carry out different tasks from a distant workstation.[1] In force-feedback robot teleoperation systems, a user drives a robot while simultaneously feels through a master device the closeness of objects in the remote environment. There are many applications for robot teleoperation, including telemedicine, exploration, entertainment, tele-services, tele-manufacturing, among others.[2] In addition, the use of the Internet as a low-cost communication channel increases the applications of these systems. However, the presence of time delays can induce instability or low performance[3–5] as well as poor transparency.[6]

There are many control schemes for standard teleoperation between two manipulators with time delay.[3] For example, Anderson and Spong[7] proposed to send scattering signals to transform the transmission delays into a passive transmission line. In refs. [8] and [9], wave transformations are used to keep the passivity of the two-port channel in front of time delay. These strategies inject the so-called apparent damping, concept extended through the time-domain passivity approach (TDPA), which is formed by a passivity observer (PO) and a passivity controller (PC),[10] where the sufficient damping to assure passivity is set depending on PO. On the other hand, in ref. [11] a simple PD-like scheme that does not require scattering or wave variable transformations yields a stable operation, including the position coordination. From this, Nuno *et al.*[12] and Hua and Liu[13] proved asymptotic stability of PD-like schemes by using a sufficiently large damping injected into the master and slave for the case of constant delays and asymmetric time-varying delays, respectively. Recently, in ref. [14], a reaction model of human operator is included in the teleoperation system to decrease the necessary damping to achieve stability.

On the other hand, the state of the art for delayed mobile robot teleoperation will generally inherit the mentioned strategies, but many times the mismatch between the models of the master and slave adds problems in the theoretical analysis. For example, if the master does not move, the mobile robot generally goes at a constant speed. The proposed strategies include compensation based on a human operator model,[15] control based on virtual-mass plus wave variable,[16] event-based control,[17] signals fusion,[18] control based on variable force-feedback gain depending on the robot–obstacle distance and

* Corresponding author. E-mail: slawinski@inaut.unsj.edu.ar

its variation in time,[19] control based on virtual force,[20] impedance control,[21] control based on the *r*-passivity,[22,23] and TDPA,[24] where different types of force feedback can be considered under a novel general framework, which is based on computing the system energy from the integration of power signals on local and remote sites to set a time-varying damping. In spite of of achieving passivity, the force feedback computed in practice is noisy, which affects the level of transparency and user's tactile perception adversely. Recently, the concept of absolute transparency was proposed for bilateral teleoperation of wheeled robots to analyze such features.[25]

In spite of the state of the art available today, it is not yet totally clear how methodologically set in a simple way the parameters of a control scheme for bilateral teleoperation of mobile robots, i.e., what parameters can be freely set and what parameters must hold some conditions in order to assure stability depending on the time delay, dynamics, independent parameters, etc. Thus, the state of the art in control design for the bilateral teleoperation of mobile robots still should be enhanced. In this context, this paper aims to introduce an approach to stable bilateral teleoperation system of mobile robots, taking advantage of the simplicity and robustness of both PD-like controller and impedance loop. From the stability analysis carried out in this paper and practical issues, a straightforward procedure to tune the control parameters is provided. The proposed control scheme includes a velocity PD-like control plus impedance at the remote site, and damping and a force feedback based on the synchronization error at the local site. This work analyzes the Lyapunov–Krasovskii stability considering the dynamics of the master and mobile robot as well as time-varying and asymmetric delays. Furthermore, the controller is evaluated from tests where a human operator drives a real mobile robot to follow a reference path avoiding collisions with the objects present in the environment. These experiments are made to verify the achieved theoretical analysis.

The paper is organized as follows: Section 2 presents some preliminary aspects such as the master and slave dynamic models and properties, assumptions and lemmas. In Section 3, a control scheme applied to bilateral teleoperation of unicycle-like wheeled robots is proposed. The stability analysis based on the Lyapunov–Krasovskii functionals is carried out in Section 4. Section 5 shows experimental results, where a user drives a wheeled robot; and finally, in section 6, the conclusions of this work are given.

2. Preliminary

This paper will analyze teleoperation systems in which a human operator drives a wheeled robot while he or she feels the environment near the robot through visual and force feedback. For example, the user could feel the closeness of an object with respect to the mobile robot, which is remotely driven using velocity commands generated by the master position.

Notation: We use standard notations throughout the paper. If x is a scalar, $\mathbf{x}$ is a vector, and $\mathbf{X}$ is a matrix, then $|x|$ is the absolute value of x, $\mathbf{x}^{\mathrm{T}}$ is the transpose of the vector, $\mathbf{X}^{\mathrm{T}}$ is the transpose of the matrix, $|\mathbf{x}|$ is the Euclidean norm of $\mathbf{x}$, $|\mathbf{X}|$ is the induced norm of $\mathbf{X}$, $\mathbf{X} > 0$ ($\mathbf{X} < 0$) means that $\mathbf{X}$ is positive definite (negative definite), and $\lambda_{\min}(\mathbf{X})$ and $\lambda_{\max}(\mathbf{X})$ represent the minimum and maximum eigen value of matrix $\mathbf{X}$, respectively. In addition, $\|\mathbf{x}\|_1$ and $\|\mathbf{x}\|_2$ represent the L1- and L2-norms of $\mathbf{x}$, respectively.

The typical nonlinear dynamic model in Cartesian coordinates is used to represent the master or local device, that is

$$\mathbf{M_m}(\mathbf{x_m})\ddot{\mathbf{x}}_\mathbf{m} + \mathbf{C_m}(\mathbf{x_m}, \dot{\mathbf{x}}_\mathbf{m})\dot{\mathbf{x}}_\mathbf{m} + \mathbf{g_m}(\mathbf{x_m}) = \mathbf{f_m} + \mathbf{f_h}, \tag{1}$$

where $\mathbf{x_m}(t) \in R^{n\times 1}$ is the end-effector position, $\dot{\mathbf{x}}_\mathbf{m}(t) \in R^{n\times 1}$ is the end-effector velocity, $\mathbf{M_m}(\mathbf{x_m}) \in R^{n\times n}$ is the inertia matrix, $\mathbf{C_m}(\mathbf{x_m}, \dot{\mathbf{x}}_\mathbf{m}) \in R^{n\times n}$ is the matrix representing centripetal and Coriolis torques, $\mathbf{g_m}(\mathbf{x_m}) \in R^{n\times 1}$ is the gravitational torque, $\mathbf{f_h} \in R^{n\times 1}$ is the human operator force, and $\mathbf{f_m} \in R^{n\times 1}$ is the control force applied to the master.

For the case of wheeled robot teleoperation, the dynamic model of a unicycle-type mobile robot is considered.[22] It has two independently actuated rear wheels, and is represented by

$$\mathbf{D}\dot{\boldsymbol{\eta}} + \mathbf{Q}(\boldsymbol{\eta})\boldsymbol{\eta} = \mathbf{f_s} + \mathbf{f_e}, \tag{2}$$

https://doi.org/10.1017/S0263574715000223 Published online by Cambridge University Press

where $\boldsymbol{\eta} = \left[\begin{smallmatrix} v \\ \omega \end{smallmatrix}\right]$ is the robot velocity vector, with v and ω representing the linear and angular velocity of the mobile robot, respectively, $\mathbf{f_e} \in R^{n\times 1}$ is the force caused by the elements of the environment on the robot, $\mathbf{D} = \left[\begin{smallmatrix} m & 0 \\ 0 & i \end{smallmatrix}\right]$ is the inertia matrix, and $\mathbf{Q} = \left[\begin{smallmatrix} 0 & -ma\omega \\ ma\omega & 0 \end{smallmatrix}\right]$ is the Coriolis matrix; m is the mass of the robot, i is the rotational inertia, and a is the distance between the mass center and the geometric center. In addition, $\mathbf{f_s} = \left[\begin{smallmatrix} u_1 \\ u_2 \end{smallmatrix}\right]$ involves a control force u_1 and a control torque u_2, with $u_1 = \frac{1}{r_w}(u_{\text{left}} + u_{\text{right}})$ and $u_2 = \frac{c}{r_w}(u_{\text{right}} - u_{\text{left}})$, where $r_w > 0$ is the radius of the wheels, $c > 0$ is the half-width of the cart, and u_{left} and u_{right} are the torques of the left and right rear wheels, respectively. Furthermore, the communication channel adds a forward time delay h_1 (from the master to the slave) and a backward time delay h_2 (from the slave to the master). Generally, these delays are time varying and have difference between them (asymmetric delays).

On the other hand, the following ordinary properties, assumptions, and lemmas will be used in this paper[11,12]:

Property 1**:** *The inertia matrices* $\mathbf{M_m}(\mathbf{x_m})$ and $\mathbf{D}$ are symmetric positive definite. The Matrix $\mathbf{D}$ is assumed constant.

Property 2: *The matrix* $\dot{\mathbf{M}}_\mathbf{m}(\mathbf{x_m}) - 2\mathbf{C_m}(\mathbf{x_m}, \dot{\mathbf{x}}_\mathbf{m})$ is skew-symmetric.

Property 3: *There exists a* $k_r > 0$ such that $\mathbf{C_m}(\mathbf{x_m},\ \dot{\mathbf{x}}_\mathbf{m})\dot{\mathbf{x}}_\mathbf{m} \leq k_r|\dot{\mathbf{x}}_\mathbf{m}|$ for all t.

Assumption 1: *The time delays* $h_1(t)$ *and* $h_2(t)$ *are bounded. Therefore, there exist positive scalars* $\bar{h}_1$ *and* $\bar{h}_2$ *such that* $0 \leq h_1(t) \leq \bar{h}_1$ *and* $0 \leq h_2(t) \leq \bar{h}_2$ for all t.

Assumption 2[26,27]: The human operator and the environment behave in a non-passive way and these are represented by the following simplified models:

$$\mathbf{f_h} = -\alpha_h \dot{\mathbf{x}}_\mathbf{m} + \mathbf{f}_{a_h}, \tag{3}$$

$$\mathbf{f_e} = -\alpha_e \boldsymbol{\eta} + \mathbf{f}_{a_e}, \tag{4}$$

where α_h is the damping of the human operator model, and α_e is the environment's damping (passive components). On the other hand, $\mathbf{f}_{a_h}$ and $\mathbf{f}_{a_e}$ are the non-passive components of these (usually called exogenous forces), which are assumed bounded, that is $|\mathbf{f_{a_h}}| \leq \bar{f}_{a_h}$ and $|\mathbf{f_{a_e}}| \leq \bar{f}_{a_e}$, with $\bar{f}_{a_h}$ and $\bar{f}_{a_e}$ being the positive constants.

Lemma 1.[12] *For real vector functions* $\mathbf{a}(.)$ and $\mathbf{b}(.)$ and a time-varying scalar $h(t)$ with $0 \leq h(t) \leq \bar{h}$, the following inequality holds:

$$-2\mathbf{a}^T(t)\int_{t-h(t)}^{t} \mathbf{b}(\xi)d\xi - \int_{t-h(t)}^{t} \mathbf{b}^T(\xi)\mathbf{b}(\xi)\,d\xi \leq h(t)\,\mathbf{a}^T(t)\,\mathbf{a}(t) \leq \bar{h}(t)\,\mathbf{a}^T(t)\,\mathbf{a}(t). \tag{5}$$

In the next section, the control scheme will be introduced.

3. PD-like Controller for Teleoperation

The PD-like controllers are simple structures that generally have a good performance in practice for common applications and are calibrated quickly. Lately, the performance of these schemes was evaluated for the position control in bilateral teleoperation systems of manipulator robots.[11,12] In these cases, if the damping of the master and the slave are sufficiently big, then the stability is assured. If the damping increases, the system is better in terms of stability but the transparency is the worst.[12]

Here, the teleoperation system is used to control the velocity of a mobile robot, where the user permanently sends commands and perceives by means of a force feedback the objects near the robot. The proposed control scheme establishes the control actions as follows:

$$\begin{cases} \mathbf{f_m} = -k_m\left(k_g\mathbf{x_m}(t) - \boldsymbol{\eta}(t-h_2)\right) - \alpha_m\dot{\mathbf{x}}_\mathbf{m} - k_p\dot{\mathbf{x}}_\mathbf{m} + \mathbf{g_m}(\mathbf{x_m}) \\ \mathbf{f_s} = k_s\left(k_g\mathbf{x_m}(t-h_1) - \boldsymbol{\eta} - k_z\mathbf{f_v}\right) - \sigma_s\mathbf{z} + \mathbf{Q}(\boldsymbol{\eta})\,\boldsymbol{\eta} \end{cases}, \tag{6}$$

https://doi.org/10.1017/S0263574715000223 Published online by Cambridge University Press

where the controller is formed by $\mathbf{f_m}$ and $\mathbf{f_s}$. The parameters k_s and σ_s are positive constants and represent the proportional gain- and acceleration-dependent damping added by the velocity controller, α_m and k_p are the damping and the spring injected in the master, respectively, k_m represents the relative spring depending on the mismatch between the master reference and the mobile robot velocity, and k_z represents the impedance applied to the virtual force $\mathbf{f_v}$, which is generated by the obstacles near the robot. Last force is assumed to be bounded by $|\mathbf{f_v}| \leq \bar{f}_v$, and will be described in Section 5.

Besides, the parameter k_g linearly maps the master position to a velocity reference, and $\mathbf{z}$ is defined by

$$\dot{\boldsymbol{\eta}} = \mathbf{z} + \gamma \dot{\mathbf{z}} \tag{7}$$

with $\gamma \to 0^+$. The signal $\mathbf{z}$ represents the mobile robot acceleration $\dot{\boldsymbol{\eta}}$ at an infinitesimal time instant before t, so it is assumed that $\dot{\boldsymbol{\eta}} \approx \mathbf{z}$, considering $\dot{\mathbf{z}}$ without discontinuities.

Next, the stability of the delayed bilateral teleoperation system modeled by (1), (2), (3), and (4), the communication channel, and the PD-like controller (6) will be analyzed.

4. Stability of the Delayed Closed-Loop System

The stability analysis is based on the Lyapunov–Krasovskii theory. It is important to remark that there is no equilibrium point but a Krasovskii-like equilibrium solution that depends on the state in the time interval $[t - h_1 - h_2, t]$. Now we present the main result of this work, which is as follows.

Theorem 1. Consider a delayed teleoperation system where a human operator (3) using a master device (1) drives a remote mobile robot described by (2) and (7), interacting with an environment (4) and including the control law (6). For positive constant parameters k_m, k_s, k_g, considering Assumptions **1**, **2**, and **3** and Properties **1**, **2**, and **3**, if the control parameters α_m and σ_s are such that the following inequalities hold:

$$-\lambda_m = -\alpha_m + \bar{h}_1 + \frac{1}{4}\bar{h}_2 k_m^2 < 0,$$

$$-\lambda_s = \frac{k_m}{k_s k_g}(-\sigma_s - |\mathbf{D}|) + \frac{1}{4}\bar{h}_1 \frac{k_m^2}{k_g^2} + \bar{h}_2 < 0,$$

then the state defined by $\boldsymbol{\theta} := [\,\mathbf{x_m}\ \dot{\mathbf{x}}_\mathbf{m}\ k_g\mathbf{x_m} - \boldsymbol{\eta}\ \mathbf{z}\ \boldsymbol{\eta}\,] \in L_\infty$. In addition, the variables $\dot{\mathbf{x}}_\mathbf{m}$ and $\mathbf{z}$ are ultimately bounded with ultimate bound given by $\max(\frac{\rho_m}{\lambda_m}, \frac{\rho_s}{\lambda_s})$, where $\rho_m = \bar{f}_{a_h}$ and $\rho_s = \frac{k_m}{k_s k_g}(\bar{f}_{a_e} + k_z \bar{f}_v)$.

Proof. First, a functional $\mathrm{V} = \mathrm{V}_1 + \mathrm{V}_2 + \mathrm{V}_3 + \mathrm{V}_4 + \mathrm{V}_5 + \mathrm{V}_6 > 0$ is proposed to analyze its evolution along the system's trajectories. The first five sub-functionals depend on the variables of $\mathbf{x}$, and are defined in the following manner:

$$V_1 = \frac{1}{2}\dot{\mathbf{x}}_\mathbf{m}^\mathbf{T}\mathbf{M_m}(\mathbf{x_m})\dot{\mathbf{x}}_\mathbf{m}, \tag{8}$$

$$V_2 = \frac{1}{2}\frac{k_m}{k_g}\left(k_g\mathbf{x_m} - \boldsymbol{\eta}\right)^\mathbf{T}\left(k_g\mathbf{x_m} - \boldsymbol{\eta}\right), \tag{9}$$

$$V_3 = \frac{1}{2}\alpha_e \frac{k_m}{k_s k_g}\boldsymbol{\eta}^\mathbf{T}\boldsymbol{\eta}, \tag{10}$$

$$V_4 = \frac{1}{2}\gamma \frac{k_m}{k_s k_g}\mathbf{z}^\mathbf{T}\mathbf{D}\mathbf{z}, \tag{11}$$

$$V_5 = \frac{1}{2}k_p\mathbf{x}_\mathbf{m}^\mathbf{T}\mathbf{x_m}. \tag{12}$$

https://doi.org/10.1017/S0263574715000223 Published online by Cambridge University Press

The time derivative of V_1 (8) along the master dynamics (1), taking into account properties **1** and **2**, is the following one:

$$\begin{aligned}\dot{\mathrm{V}}_1 &= \frac{1}{2}\dot{\mathbf{x}}_\mathbf{m}{}^\mathbf{T}\dot{\mathbf{M}}_\mathbf{m}\dot{\mathbf{x}}_\mathbf{m} + \dot{\mathbf{x}}_\mathbf{m}{}^\mathbf{T}\mathbf{M}_\mathbf{m}\ddot{\mathbf{x}}_\mathbf{m} \\ &= \frac{1}{2}\dot{\mathbf{x}}_\mathbf{m}{}^\mathbf{T}\dot{\mathbf{M}}_\mathbf{m}\dot{\mathbf{x}}_\mathbf{m} + \dot{\mathbf{x}}_\mathbf{m}{}^\mathbf{T}\mathbf{M}_\mathbf{m}\mathbf{M}_\mathbf{m}^{-\mathbf{1}}\left(\boldsymbol{\tau}_\mathbf{m} + \mathbf{f}_\mathbf{h} - \mathbf{g}\left(\mathbf{x}_\mathbf{m}\right) - \mathbf{C}_\mathbf{m}\dot{\mathbf{x}}_\mathbf{m}\right) \\ &= \dot{\mathbf{x}}_\mathbf{m}{}^\mathbf{T}\left(\boldsymbol{\tau}_\mathbf{m} + \mathbf{f}_\mathbf{h} - \mathbf{g}\left(\mathbf{x}_\mathbf{m}\right)\right). \end{aligned} \tag{13}$$

Now, if the control action $\mathbf{f}_\mathbf{m}$ of (6) is included in (13) considering also (3), it yields,

$$\begin{aligned}\dot{\mathrm{V}}_1 &= \dot{\mathbf{x}}_\mathbf{m}{}^\mathbf{T}\left(\mathbf{f}_\mathbf{m} - \mathbf{g}_\mathbf{m}\left(\mathbf{x}_\mathbf{m}\right)\right) + \dot{\mathbf{x}}_\mathbf{m}{}^\mathbf{T}\mathbf{f}_\mathbf{h} \\ &= \dot{\mathbf{x}}_\mathbf{m}{}^\mathbf{T}\left(-k_m\left(k_g\mathbf{x}_\mathbf{m} - \boldsymbol{\eta}\left(t-h_2\right)\right) - \alpha_m\dot{\mathbf{x}}_\mathbf{m}\right) + \dot{\mathbf{x}}_\mathbf{m}{}^\mathbf{T}\left(\mathbf{f}_{\mathbf{a}_\mathbf{h}} - \alpha_h\dot{\mathbf{x}}_\mathbf{m} - k_p\mathbf{x}_\mathbf{m}\right) \\ &= -k_m\dot{\mathbf{x}}_\mathbf{m}{}^\mathbf{T}\left(\left(k_g\mathbf{x}_\mathbf{m} - \boldsymbol{\eta}\left(t-h_2\right) + \boldsymbol{\eta} - \boldsymbol{\eta}\right)\right) - \left(\alpha_m + \alpha_h\right)\dot{\mathbf{x}}_\mathbf{m}{}^\mathbf{T}\dot{\mathbf{x}}_\mathbf{m} - k_h\dot{\mathbf{x}}_\mathbf{m}{}^\mathbf{T}\mathbf{x}_\mathbf{m} + \dot{\mathbf{x}}_\mathbf{m}{}^\mathbf{T}\mathbf{f}_{\mathbf{a}_\mathbf{h}} \\ &= -\left(\alpha_m + \alpha_h\right)\dot{\mathbf{x}}_\mathbf{m}{}^\mathbf{T}\dot{\mathbf{x}}_\mathbf{m} - k_m\dot{\mathbf{x}}_\mathbf{m}{}^\mathbf{T}\left(k_g\mathbf{x}_\mathbf{m} - \boldsymbol{\eta}\right) - k_m\dot{\mathbf{x}}_\mathbf{m}{}^\mathbf{T}\int_{t-h_2}^{t}\dot{\boldsymbol{\eta}}\left(\xi\right)d\xi - k_p\dot{\mathbf{x}}_\mathbf{m}{}^\mathbf{T}\mathbf{x}_\mathbf{m} + \dot{\mathbf{x}}_\mathbf{m}{}^\mathbf{T}\mathbf{f}_{\mathbf{a}_\mathbf{h}} \end{aligned} \tag{14}$$

Next, $\dot{\mathrm{V}}_2$ is obtained from (9) considering $\mathbf{z} \approx \dot{\boldsymbol{\eta}}$ from (7), as follows:

$$\dot{\mathrm{V}}_2 = \frac{k_m}{k_g}\left(k_g\mathbf{x}_\mathbf{m} - \boldsymbol{\eta}\right)^\mathbf{T}\left(k_g\dot{\mathbf{x}}_\mathbf{m} - \dot{\boldsymbol{\eta}}\right) \approx -\frac{k_m}{k_g}\left(k_g\mathbf{x}_\mathbf{m} - \boldsymbol{\eta}\right)^\mathbf{T}\mathbf{z} + k_m\left(k_g\mathbf{x}_\mathbf{m} - \boldsymbol{\eta}\right)^\mathbf{T}\dot{\mathbf{x}}_\mathbf{m}. \tag{15}$$

On the other hand, $\dot{\mathrm{V}}_3$ is computed from (10) taking into account $\mathbf{z} \approx \dot{\boldsymbol{\eta}}$ from (7), as follows:

$$\dot{\mathrm{V}}_3 = \alpha_e\frac{k_m}{k_sk_g}\boldsymbol{\eta}^\mathbf{T}\dot{\boldsymbol{\eta}} \approx \alpha_e\frac{k_m}{k_sk_g}\boldsymbol{\eta}^\mathbf{T}\mathbf{z}. \tag{16}$$

Besides, $\dot{\mathrm{V}}_4$ along the mobile robot dynamics (2) can be written, including (6) into the derivative of (11), in the following way:

$$\begin{aligned}\dot{\mathrm{V}}_4 &= \gamma\frac{k_m}{k_sk_g}\mathbf{z}^\mathbf{T}\mathbf{D}\dot{\mathbf{z}} = \gamma\frac{k_m}{k_sk_g}\mathbf{z}^\mathbf{T}\mathbf{D}\left(\frac{\dot{\boldsymbol{\eta}}}{\gamma} - \frac{\mathbf{z}}{\gamma}\right) \\ &= \frac{k_m}{k_sk_g}\mathbf{z}^\mathbf{T}\mathbf{D}\dot{\eta} - \frac{k_m}{k_sk_g}\mathbf{z}^\mathbf{T}\mathbf{D}\mathbf{z} \\ &= -\sigma_s\frac{k_m}{k_sk_g}\mathbf{z}^\mathbf{T}\mathbf{z} + \frac{k_m}{k_sk_g}\mathbf{z}^\mathbf{T}\left(\mathbf{f}_\mathbf{e} + k_z\mathbf{f}_\mathbf{v}\right) - \frac{k_m}{k_sk_g}\mathbf{z}^\mathbf{T}\mathbf{D}\mathbf{z} \\ &\quad + \frac{k_m}{k_g}\mathbf{z}^\mathbf{T}\left(k_g\mathbf{x}_\mathbf{m}\left(t-h_1\right) + \mathbf{x}_\mathbf{m} - \mathbf{x}_\mathbf{m} - \boldsymbol{\eta}\right) \\ &= -\sigma_s\frac{k_m}{k_sk_g}\mathbf{z}^\mathbf{T}\mathbf{z} + \frac{k_m}{k_g}\mathbf{z}^\mathbf{T}\left(k_g\mathbf{x}_\mathbf{m} - \boldsymbol{\eta}\right) - \alpha_e\frac{k_m}{k_sk_g}\mathbf{z}^\mathbf{T}\boldsymbol{\eta} \\ &\quad + \frac{k_m}{k_sk_g}\mathbf{z}^\mathbf{T}\left(\mathbf{f}_{\mathbf{a}_\mathbf{e}} + k_z\mathbf{f}_\mathbf{v}\right) - \frac{k_m}{k_sk_g}\mathbf{z}^\mathbf{T}\mathbf{D}\mathbf{z} - \frac{k_m}{k_g}\mathbf{z}^\mathbf{T}\int_{t-h_1}^{t}\dot{\mathbf{x}}_\mathbf{m}\left(\xi\right)d\xi. \end{aligned} \tag{17}$$

Furthermore, $\dot{\mathrm{V}}_5$ is obtained from (12) as follows:

$$\dot{\mathrm{V}}_5 = k_p\mathbf{x}_\mathbf{m}{}^\mathbf{T}\dot{\mathbf{x}}_\mathbf{m}. \tag{18}$$

https://doi.org/10.1017/S0263574715000223 Published online by Cambridge University Press

It is possible to appreciate in (14) and (17) that there are terms with delayed variables that make the stability analysis difficult. To solve this, V_6 is proposed as follows:

$$V_6 = \int_{-\bar{h}_2}^{0} \int_{t+\theta}^{t} \mathbf{z}(\xi)^{\mathbf{T}} \mathbf{z}(\xi) d\xi d\theta + \int_{-\bar{h}_1}^{0} \int_{t+\theta}^{t} \dot{\mathbf{x}}_{\mathbf{m}}(\xi)^{\mathbf{T}} \dot{\mathbf{x}}_{\mathbf{m}}(\xi) d\xi d\theta. \tag{19}$$

From (19), and considering Assumption **1**, $\dot{\mathrm{V}}_6$ is computed as

$$\dot{\mathrm{V}}_6 \leq \bar{h}_2 \mathbf{z}^{\mathbf{T}} \mathbf{z} - \int_{t-h_2}^{t} \mathbf{z}^{\mathbf{T}}(\xi) \mathbf{z}(\xi) d\xi + \bar{h}_1 \dot{\mathbf{x}}_{\mathbf{m}}{}^{\mathbf{T}} \dot{\mathbf{x}}_{\mathbf{m}} - \int_{t-h_1}^{t} \dot{\mathbf{x}}_{\mathbf{m}}{}^{\mathbf{T}}(\xi) \dot{\mathbf{x}}_{\mathbf{m}}(\xi) d\xi. \tag{20}$$

The terms with integrals in (20) can be linked with the third term in (14) and the sixth term in (17) by using Lemma 1 (5), and considering (7), it yields,

$$-\frac{k_m}{k_g} \mathbf{z}^{\mathbf{T}} \int_{t-h_1}^{t} \dot{\mathbf{x}}_{\mathbf{m}}(\xi) d\xi - \int_{t-h_1}^{t} \dot{\mathbf{x}}_{\mathbf{m}}{}^{\mathbf{T}}(\xi) \dot{\mathbf{x}}_{\mathbf{m}}(\xi) d\xi \leq \frac{1}{4} \bar{h}_1 \frac{k_m^2}{k_g^2} \mathbf{z}^{\mathbf{T}} \mathbf{z}, \tag{21}$$

$$\begin{aligned} &- \int_{t-h_2}^{t} \mathbf{z}^{\mathbf{T}}(\xi) \mathbf{z}(\xi) d\xi - k_m \dot{\mathbf{x}}_{\mathbf{m}}{}^{\mathbf{T}} \int_{t-h_2}^{t} \dot{\boldsymbol{\eta}}(\xi) d\xi = - \int_{t-h_2}^{t} \mathbf{z}^{\mathbf{T}}(\xi) \mathbf{z}(\xi) d\xi - k_m \dot{\mathbf{x}}_{\mathbf{m}}{}^{\mathbf{T}} \\ &\times \int_{t-h_2}^{t} (\mathbf{z}(\xi) + \gamma \dot{\mathbf{z}}(\xi)) d\xi \leq \frac{1}{4} \bar{h}_2 k_m^2 \dot{\mathbf{x}}_{\mathbf{m}}{}^{\mathbf{T}} \dot{\mathbf{x}}_{\mathbf{m}} - \gamma k_m \dot{\mathbf{x}}_{\mathbf{m}}{}^{\mathbf{T}} \int_{t-h_2}^{t} \dot{\mathbf{z}}(\xi) d\xi. \end{aligned} \tag{22}$$

In the last term of (22), the integral function is applied in a closed interval to $\dot{\mathbf{z}}(t)$ (assumed without discontinuities), so the function $\int_{t-h_2}^{t} \dot{\mathbf{z}}(\xi) d\xi$ has a maximum real value β that bounds such function and therefore holds $|\int_{t-h_2}^{t} \dot{\mathbf{z}}(\xi) d\xi| \leq h_2 \beta$. From this, (22) can be rewritten as,

$$\frac{1}{4} \bar{h}_2 k_m^2 \dot{\mathbf{x}}_{\mathbf{m}}{}^{\mathbf{T}} \dot{\mathbf{x}}_{\mathbf{m}} - \gamma k_m \dot{\mathbf{x}}_{\mathbf{m}}{}^{\mathbf{T}} \int_{t-h_2}^{t} \dot{\mathbf{z}}(\xi) d\xi \leq \frac{1}{4} \bar{h}_2 k_m^2 \dot{\mathbf{x}}_{\mathbf{m}}{}^{\mathbf{T}} \dot{\mathbf{x}}_{\mathbf{m}} + k_m \gamma \beta \bar{h}_2 |\dot{\mathbf{x}}_{\mathbf{m}}|, \tag{23}$$

that is, the terms with integrals were replaced by common quadratic terms. Finally, $\dot{\mathrm{V}}$can be built joining (14), (15), (16), (17), (18), and (20), considering $k_m \gamma \beta \bar{h}_2 \to 0$ and the relations (21) and (23) as follows:

$$\begin{aligned} \dot{\mathrm{V}} &= \dot{\mathrm{V}}_1 + \dot{\mathrm{V}}_2 + \dot{\mathrm{V}}_3 + \dot{\mathrm{V}}_4 + \dot{\mathrm{V}}_5 \\ &\leq \dot{\mathbf{x}}_{\mathbf{m}}{}^{\mathbf{T}} \left[-\alpha_m \mathbf{I} + \bar{h}_1 \mathbf{I} + \frac{1}{4} \bar{h}_2 k_m^2 \mathbf{I} \right] \dot{\mathbf{x}}_{\mathbf{m}} + \mathbf{z}^{\mathbf{T}} \left[\frac{k_m}{k_s k_g} (-\sigma_s \mathbf{I} - \mathbf{D}) + \frac{1}{4} \bar{h}_1 \frac{k_m^2}{k_g^2} \mathbf{I} + \bar{h}_2 \mathbf{I} \right] \mathbf{z} \\ &+ \frac{k_m}{k_s k_g} \left(\bar{f}_{a_e} + k_z \bar{f}_v \right) |\mathbf{z}| + \bar{f}_{a_h} |\dot{\mathbf{x}}_{\mathbf{m}}| \\ &= -\lambda_m \dot{\mathbf{x}}_{\mathbf{m}}{}^{\mathbf{T}} \dot{\mathbf{x}}_{\mathbf{m}} - \lambda_s \mathbf{z}^{\mathbf{T}} \mathbf{z} + \rho_m |\dot{\mathbf{x}}_{\mathbf{m}}| + \rho_s |\mathbf{z}|. \end{aligned} \tag{24}$$

Given positive constant parameters for k_m, k_s, and k_g, as well as bounded values for $\bar{h}_1$, $\bar{h}_2$, $\bar{f}_{a_e}$, and $\bar{f}_{a_h}$, the control parameters α_m and σ_s can be set to guarantee that the first two terms of (24) are negative definite, and therefore $\boldsymbol{\theta} \in L_\infty$. For this condition, it is possible to appreciate from (24) that the state variables $\dot{\mathbf{x}}_{\mathbf{m}}$ and $\mathbf{z}$ are ultimately bounded with ultimate bound $\max(\frac{\rho_m}{\lambda_m}, \frac{\rho_s}{\lambda_s})$. The proof is completed.•

Remark 1. If the active components of the human operator $\mathbf{f}_{\mathbf{a_h}}$, the environment $\mathbf{f}_{\mathbf{a_e}}$, and the fictitious force $\mathbf{f}_{\mathbf{v}}$ are null ($\bar{f}_{a_h} = \bar{f}_{a_e} = \bar{f}_v = 0$), then $\rho_m = \rho_s = 0$ and therefore the system is stable. For this particular case, Barbalat's lemma can be used in (24); taking into account Assumptions **1**, **2**, and **3**, Property **3,** and the fact that $[\, \mathbf{x}_{\mathbf{m}} \; \dot{\mathbf{x}}_{\mathbf{m}} \; k_g \mathbf{x}_{\mathbf{m}} - \boldsymbol{\eta} \; \mathbf{z} \; \boldsymbol{\eta} \,] \in L_\infty$; it is possible to deduce that $\ddot{\mathbf{x}}_{\mathbf{m}}$ and $\dot{\mathbf{z}}$ are bounded, and consequently $\ddot{V}$ is bounded too. Then, $\dot{\mathbf{x}}_{\mathbf{m}}$ and $\mathbf{z}$ will tend to zero as $t \to \infty$.

https://doi.org/10.1017/S0263574715000223 Published online by Cambridge University Press

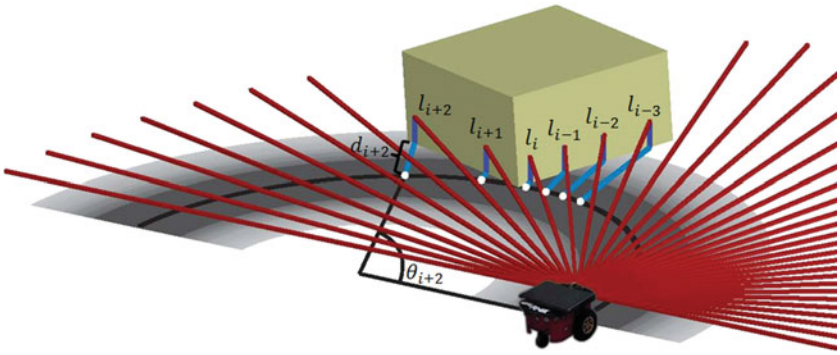

Fig. 1. Fictitious force based on 2D laser scanner and the mobile robot motion.

5. Impedance Based on Fictitious Force

This section describes how the fictitious force $\mathbf{f_v}$ is computed to be used in $\mathbf{f_s}$ (6). The virtual force $\mathbf{f_v}$ is calculated using the robot motion prediction and the data provided by a 2D laser scanner. First, the path predicted for the mobile robot considering that υ and ω remain constant, is computed. Then the 2D laser sensor gets n measurements of distance l_i between the robot and the obstacles near it. Each measure is associated to one given direction, as shown in Fig. 1. From this, the points (o_i) closer to the positions l_i on the robot's future path are obtained. The distance between o_i and l_i is named as d_i. Now, for each o_i the angle (θ_i) measured from the center point of the circumference-type path of curvature radius $r(t)$ defined by the robot velocity is obtained. Next, the distance along the path $s_i = r(t)\theta_i$ from the current position of the mobile robot to o_i is calculated.

Now a weigh factor p_i is defined depending on (d_i) as follows:

$$p_i = \begin{cases} 1 & d_i \leq c/2 \\ \dfrac{\left(1 + \cos\left(\dfrac{\pi}{\delta}\left(d_i \dfrac{c}{2}\right)\right)\right)}{2} & \dfrac{c}{2} < d_i < \delta + \dfrac{c}{2} \\ 0 & d_i \geq \delta + \dfrac{c}{2} \end{cases}, \tag{25}$$

where c is the robot width. If $d_i < \delta + \frac{c}{2}$, the robot will collide with the obstacle if it keeps its velocity vector. Otherwise p_i is decreased as the points are further away from the path. Finally, the fictitious force vector $\mathbf{f_v}$ is computed according to p_i and s_i in the following manner:

$$\mathbf{f_v} = \frac{k}{n}\left[\sum_{i=1}^{n} p_i \left(s_{\max} - s_i\right) \quad 0\right], \tag{26}$$

where n is the quantity of the measurements provided by 2D laser scanner, $s_i = r(t)\frac{\pi}{2}$, and $k > 0$ is a gain to scale the force.

6. Experimental Results

In this section, the proposed control scheme is tested. In the experiments, a human operator drives a Pioneer 2DX mobile robot employing a hand-controller with force feedback. The master device is a Novint Falcon running at 1 Khz. On the other hand, the mobile robot has incremental encoders in both DC motors and a Hokuyo 2D laser scanner to compute the fictitious force. In addition, a webcam onboard the robot is used to send visual feedback to the user. The layout of the experiment is shown in Fig. 2, where it is possible to appreciate the reference path (marked on the floor with white ribbon but enhanced in the image using a black solid line) established as a goal for the delayed bilateral teleoperation system test.

6.1. Testing methodology

The methodology used to carry out and evaluate the experiments is as follows:

https://doi.org/10.1017/S0263574715000223 Published online by Cambridge University Press

Fig. 2. Reference path for the teleoperated mobile robot.

1. The equipment used is the following: 3D master device with force feedback, mobile robot, 2D laser sensor, vision camera, and two notebooks (one onboard the robot) connected via wireless ad-hoc network. Because the network connection has a negligible delay, a delay added by software is implemented which helps to compare different setups in front of similar time delays. It is outside of the scope of this work the modeling of some specific type of time delays such as those present in communications via wi-fi, internet, etc. In this paper, the time delays are taken in a general way as variables, asymmetric and bounded magnitude.
2. The goal of the test is for a user to drive a mobile robot in order to follow a reference path avoiding two static obstacles located in the workspace, and lastly move the robot to the final position of the reference path.
3. The PD-like control scheme is evaluated for 5 different conditions. Each condition is tested for 10 times. The conditions tested are as follows:
   (a) Null both time delay and master damping.
   (b) $h_1 = 0.75 + 0.25\sin(0.2\pi t)$ and $h_2 = 1$ (both in seconds) and null master damping.
   (c) $h_1 = 0.75 + 0.25\sin(0.2\pi t)$ and $h_2 = 1$ (both in seconds) and master damping set by Theorem 1, which results in $\boldsymbol{\alpha}_\mathbf{m} = \begin{bmatrix} 58 & 0 \\ 0 & 8 \end{bmatrix}$ and $\boldsymbol{\alpha}_\mathbf{s} = \begin{bmatrix} 0.23 & 0 \\ 0 & 1.25 \end{bmatrix}$ (see Section 6.2).
   (d) $h_1 = 1.125 + 0.375\sin(0.2\pi t)$ and $h_2 = 1.5$ (both in seconds) and null master damping.
   (e) $h_1 = 1.125 + 0.375\sin(0.2\pi t)$ and $h_2 = 1.5$ (both in seconds) and master damping set by Theorem 1, which results in $\boldsymbol{\alpha}_\mathbf{m} = \begin{bmatrix} 86 & 0 \\ 0 & 11 \end{bmatrix}$ and $\boldsymbol{\alpha}_\mathbf{s} = \begin{bmatrix} 1.43 & 0 \\ 0 & 2 \end{bmatrix}$ (see Section 6.2).
4. The time-to-complete the task and the time-including-force fictitious are computed for each testing and the average values of both metrics are calculated.

6.2. Procedure to tune the control parameters

The parameters k_g, k_p, k_m, k_s, α_m, α_s in Section 3 were taken as scalars, but, in general, these can be diagonal matrices called $\mathbf{K_g}$, $\mathbf{K_p}$, $\mathbf{K_m}$, $\mathbf{K_s}$, $\boldsymbol{\alpha}_\mathbf{m}$, $\boldsymbol{\sigma}_\mathbf{s}$, respectively. The procedure proposed to set the control parameters is as follows:

1. Taking $\mathbf{K_m} = 0$ (unilateral case), and $h_1 = h_2 \approx 0$ $[s]$, set $\mathbf{K_g}$ to establish the maximum velocity command and $\mathbf{K_s}$ considering the dynamics of the mobile robot in order to get a good performance of the velocity controller. We set $\mathbf{K_g} = \begin{bmatrix} 14 & 0 \\ 0 & 14 \end{bmatrix}$ and $\mathbf{K_s} = \begin{bmatrix} 25 & 0 \\ 0 & 0.5 \end{bmatrix}$.
2. Set $\mathbf{K_m}$ to match the desired level of force feedback cue considering different gains between the master and the mobile robot. $\mathbf{K_p}$ is chosen near zero to avoid interfering with the force feedback. We set $\mathbf{K_m} = \begin{bmatrix} 15 & 0 \\ 0 & 5 \end{bmatrix}$ and $\mathbf{K_p} = \begin{bmatrix} 0.01 & 0 \\ 0 & 0.01 \end{bmatrix}$.

https://doi.org/10.1017/S0263574715000223 Published online by Cambridge University Press

Table I. Time metrics for conditions (a), (b), (c), (d), and (e).

Conditions	Average time to complete the task (s)	Average time to cross the two obstacles (s)
(a)	20.52	5.6
(b)	37.45	15.1
(c)	34.03	11.9
(d)	95.75	76.2
(e)	56.64	37.32

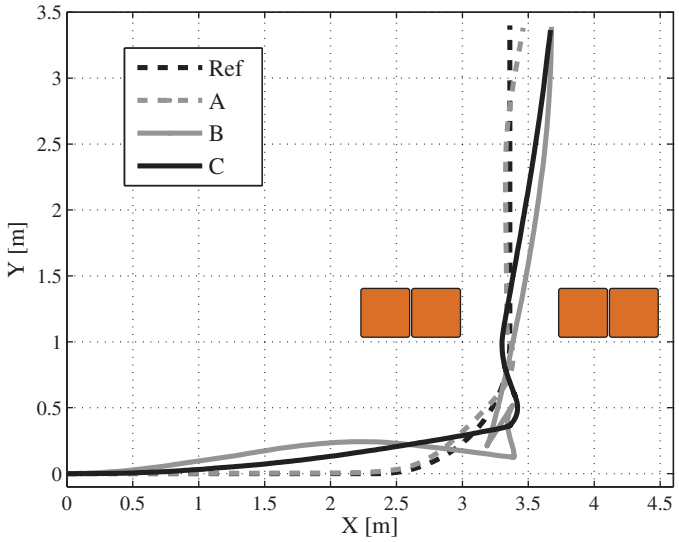

Fig. 3. Paths followed by the mobile robot for conditions (a), (b), and (c).

3. Considering the inertia matrix $\mathbf{D}$ of the robot, in this case $\mathbf{D} = \begin{bmatrix} 28.05 & 0 \\ 0 & 0.175 \end{bmatrix}$, and the maximum time delays $\bar{h}_1$ and $\bar{h}_2$, apply Theorem 1 to set $\boldsymbol{\alpha}_\mathbf{m}$, $\boldsymbol{\sigma}_\mathbf{s}$.

Remark 2. It is important to point out that there is no theoretical constraint to set parameters $\mathbf{K_g}$, $\mathbf{K_p}$, $\mathbf{K_m}$, $\mathbf{K_s}$, that is, such control parameters are independent on the time delay. On the other hand, point 3 must hold to get stability. Items 1 and 2 describe guidelines to get good performance in practice.

6.3. Results

Figure 3 shows the paths followed by the mobile robot for the conditions (a), (b), and (c). Condition (b) has more fluctuations than others because of the presence of time delay and the lack of master damping. The absence of damping causes the user to execute fast change commands, which in a delayed bilateral teleoperation loop generally produces motions with some oscillations, making difficult the action of crossing the two obstacles placed in the workspace. Table I summarizes the average time to complete the task and the average time to cross the two obstacles (non-null fictitious force). Such values show that the inclusion of damping into the master decreases the time used for condition (c) to complete the task and cross the two obstacles with respect to condition (b). Of course, the better performance is obtained with condition (a) because there is no time delay.

In Fig. 4, the evolution in time of the linear component of state variables and fictitious force for condition (c) is shown. It is important to signal that in the time interval [0, 20.1] s, the human operator drives the mobile robot speed $\boldsymbol{\eta}$ in synchronism with his command $\mathbf{x_m}$. Later, during the time interval between 20.1 and 32.6 s, the mobile robot is crossing the two obstacles, and therefore the impedance based on fictitious force increases the error $k_g\mathbf{x_m} - \boldsymbol{\eta}$. Posteriorly, the user drives the mobile robot faster to the position goal and later at 37.1 s, he or she decelerates it, stopping the mobile robot.

https://doi.org/10.1017/S0263574715000223 Published online by Cambridge University Press

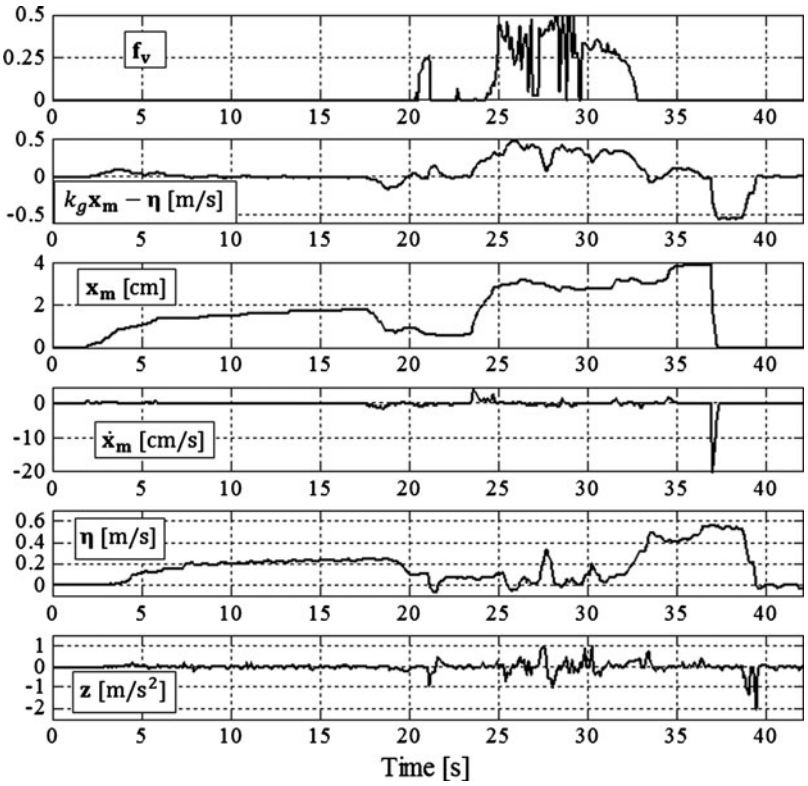

Fig. 4. Fictitious force and linear components of the state for condition (c).

Remark 3. In the experiments, the reference path marked on the floor (dashed black line in Fig. 3) is only taken as a visual guide for the human operator in order to get a better comparison in the metrics about time-to-complete the task in presence of different conditions of time delay and control parameters (see Table I). It is important to signal that the controller does not know such a reference path because it is not a path tracking controller but a bilateral scheme that helps the user for online driving the velocity of the mobile robot while simultaneously receiving force feedback.

As a result of this, there will always be a path tracking error.

7. Conclusions

In this paper, a control scheme for a mobile robot bilateral teleoperation system has been proposed considering asymmetric and time-varying delays. The stability analysis carried out gives as a result the level of necessary damping to be applied into the master and the mobile robot to assure stability of the system, mainly depending on forward and reverse time delays added by the communication channel. On the other hand, the impedance based on fictitious force helps to avoid collisions but adds a perturbation in the synchronization error, which can be felt by human operator. This perception can be used by him to modify the velocity command to decrease such error between the master position and the mobile robot velocity. In this way, the human operator can correctly control the robot receiving information through force feedback. Finally, experiments were made to validate the tuning procedure of control parameters, including set-free parameters and others depending on stability conditions. In such experiments, a Pioneer 2DX mobile robot was teleoperated by a user using a Novint Falcon joystick as a master device, where a stable behavior was achieved for different time delays. The experimental results showed bounded errors of state variables, which are in agreement with the performed theoretical analysis. But the performance worsens as the time delay rises, therefore the stability analysis should be complemented with the analysis of different human–robot interaction metrics to improve the current performance achieved in practice.

https://doi.org/10.1017/S0263574715000223 Published online by Cambridge University Press

References

1. T. B. Sheridan, *Telerobotics, Automation, and Human Supervisory Control* (MIT Press, Cambrige, MA, 1992).
2. M. Ferre, M. Buss, R. Aracil, C. Melchiorri and C. Balaguer, *Advances in Telerobotics* (Springer-Verlag, Berlin, Germany, 2007).
3. P. F. Hokayem and M. W. Spong, "Bilateral teleoperation: An historical survey," *Automatica* **42**, 2035–2057 (2006).
4. J. P. Richard, "Time-delay systems: An overview of some recent advances and open problems," *Automatica* **39**, 1667–1694 (2003).
5. T. B. Sheridan, "Space teleoperation through time delay: Review and prognosis," *IEEE Trans. Robot. Autom.* **9**(5), 592–606 (Oct. 1993).
6. D. A. Lawrence, "Stability and transparency in bilateral teleoperation," *IEEE Trans. Robot. Autom.* **9**, 624–637 (Oct. 1993).
7. R. J. Anderson and M. Spong, "Bilateral control of teleoperators with time delay," *IEEE Trans. Autom. Control* **34**(5), 494–501 (1989).
8. G. Niemeyer and J. J. E. Slotine, "Stable adaptive teleoperation," *IEEE J. Ocean Eng.* **16**(1), 152–162 (1991).
9. G. Niemeyer and J. Slotine, "Telemanipulation with time delays," *Int. J. Robot. Res.* **23**(9), 873–890 (2004).
10. J. H. Ryu, J. Artigas and C. Preusche, "A passive bilateral control scheme for a teleoperator with time-varying communication delay," *Mechatronics* **20**(7), 812823 (2010).
11. D. Lee and M. Spong, "Passive bilateral teleoperation with constant time delay," *IEEE Trans. Robot.* **22**(2), 269–281 (Apr. 2006).
12. E. Nuno, R. Ortega, N. Barabanov and L. Basanez, "A globally stable PD controller for bilateral teleoperators," *IEEE Trans. Robot.* **22**(3), 753–758 (2008).
13. C.-C. Hua and X. P. Liu, "Delay-dependent stability criteria of teleoperation systems with asymmetric time-varying delays," *IEEE Trans. Robot.* **26**(5), 925–932 (Oct. 2010).
14. E. Slawiñski and V. Mut, "PD-like controllers for delayed bilateral teleoperation of manipulators robots," *Int. J. Robust Nonlinear Control* (article first published online: Apr. 4, 2014), doi:10.1002/rnc.3177.
15. E. Slawinski, V. Mut and J. F. Postigo, "Teleoperation of mobile robots with time-varying delay," *IEEE Trans. Robot.* **23**(5), 1071–1082 (2007).
16. Z. Xu, L. Ma and K. Schilling, "Passive Bilateral Teleoperation of a Car-Like Mobile Robot," *Proceedings of the 17th Mediterranean Conference on Control & Automation*, Thessaloniki, Greece (Jun. 24–26, 2009) pp. 790–796.
17. I. Elhajj, N. Xi, W. K. Fung, Y.-H. Liu, Y. Hasegawa and T. Fukuda, "Supermedia-enhanced internet-based telerobotics," *Proc. IEEE* **91**(3), 396–421 (Mar. 2003).
18. E. Slawiñski, V. Mut, L. Salinas and S. García, "Teleoperation of a mobile robot with time-varying delay and force feedback," *Robotica* **30**, 67–77 (2012).
19. I. Farkhatdinov, J.-H. Ryu and J. An, "A Preliminary Experimental Study on Haptic Teleoperation of Mobile Robot with Variable Force Feedback Gain," *Proceedings of the IEEE Haptics Symposium*, Waltham, Boston, Massachusetts (Mar. 24–25, 2010) pp. 251–256.
20. N. Diolaiti and C. Melchiorri, "Haptic Teleoperation of a Mobile Robot," *Proceedings of the 7th IFAC SYROCO*, Wrocław, Poland (Sep. 1–3, 2003) pp. 2798–2805.
21. F. Janabi-Sharifi and I. Hassanzadeh, "Experimental analysis of mobile robot teleoperation via shared impedance control," *IEEE Trans. Syst. Man Cybern.* **41**(2), 591606 (Apr. 2011).
22. D. Lee, O. Martinez-Palafox and M. W. Spong, "Bilateral Teleoperation of a Wheeled Mobile Robot over Delayed Communication Network," *Proceedings of the IEEE International Conference on Robotics and Automation (ICRA)*, Orlando, Florida, USA (May 15–19, 2006) pp. 3298–3303.
23. D. Lee and D. Xu, "Feedback r-Passivity of Lagrangian Systems for Mobile Robot Teleoperation," *Proceedings of the IEEE International Conference on Robotics and Automation (ICRA)*, Shanghai, China (May 9–13, 2011) pp. 2118–2123.
24. H. V. Quang, I. Farkhatdinov and J.-H. Ryu, "Passivity of Delayed Bilateral Teleoperation of Mobile Robots with Ambiguous Causalities: Time Domain Passivity Approach," *Proceedings of the IEEE/RSJ International Conference on Intelligent Robots and Systems (IROS)*, Vilamoura-Algarve, Portugal (Oct. 7–12, 2012) pp. 2635–2640.
25. E. Slawiñski, V. Mut, P. Fiorini and L. Salinas, "Quantitative Absolute Transparency for Bilateral Teleoperation of Mobile Robots," *IEEE Trans. Syst. Man Cybern.* **42**(2), 430–442 (Mar. 2012).
26. W.-H. Zhu and S. Salcudean, "Stability guaranteed teleoperation: An adaptive motion/force control approach," *IEEE Trans. Autom. Control* **45**(11), 1951–1969 (Nov. 2000).
27. A. Shahdi and S. Sirouspour, "Adaptive/robust control for time-delay teleoperation," *IEEE Trans. Robot.* **25**(1), 196–205 (Feb. 2009).